For cited: *Hussein, M. A. & Aesa, A. A. (2022). Study of Effect the Iron arm Thickness and the Distance Between Pole Pieces on the Optical Performance of Symmetrical Double Pole Piece Magnetic lens. Journal of Current Researches on Educational Studies, 12 (2), 57-66.*

Journal of Current Researches on Educational Studies (JoCuRES)
www.jocures.com

Year: 2022
Volume: 12
Issue: 2

Crossref doi: 10.26579/jocures.12.2.5

Research Article

Study of Effect the Iron arm Thickness and the Distance Between Pole Pieces on the Optical Performance of Symmetrical Double Pole Piece Magnetic lens

Mohammed A. HUSSEİN[1] & Abdulsattar A. AESA[2]

Keywords
Objective magnetic lens, Iron arm thickness, Distance between pole piece, optical performance, symmetrical double pole piece lens.

Article History
Received
21 Apr, 2022
Accepted
30 Dec, 2022

Abstract
In this paper, a symmetrical double pole piece magnetic lens has been designed as an objective lens to be used for electron microscope. Three different thickness (t= 4, 8, 12) mm of iron arm were chosen at a constant distance of (S=2 mm) between pole piece of lens. The results show that at (t= 8 mm) of iron arm thickness, a better optical properties of lens; magnetics flux density (Bz), focal length (fo), spherical (Cs) and chromatic (Cc) aberration were achieved. Then, the effect of various value of the distance (S= 2,4,6) mm between the pole piece at a chosen thickness of iron arm was investigated. The highest magnetic flux density and low chromatic and spherical aberration coefficient were achieved at iron arm thickness and the distance between the pole piece (t= 8 mm, S= 2 mm) respectively. The optical properties of the lens as a function of accelerated voltage in the range of (Vr = 1 to 9) Volt was studied at a constant lens excitation of (NI = 2 kA-t). The distribution of magnetic flux at different excitations values was calculated.

1. Introduction

Nano- technology has been used in manufacturing the measurements devices and instruments in small size down to nanometers scale(1,2). Therefore, a high development in manufacturing of modern electron- microscope has huge impact in biological research and discovering the micro structure in life tissues and cells. The scanning electron microscope is considered as a most common instruments that used to measure and analyzing the micro structure with a high precision by using electron gun with short wavelength less than 1 nm (3,4). Generally, two types of electron microscope are available; firstly, scanning electron ,microscope, secondly, transmission electron microscope (1,3). , third type is produced by combining of two main types which isn't represent as a separated type, all these types have same main components (5). The scanning electron microscope depending on the electron gun can be divided into two types; thermal emission scanning electron microscope and field emission scanning electron microscope (6). The field

[1] Corresponding Author. ORCID: 0000-0001-8106-5233. University of Kirkuk, College of Education, Department of Physics, Kirkuk, Iraq, mohdphy@uokirkuk.edu.iq
[2] ORCID: 0000-0001-5935-547X. University of Kirkuk, College of Education, Department of Physics, Kirkuk, Iraq, a_aesa@uokirkuk.edu.iq

emission model is more preferred to achieve a high resolving power due to a small diameter of electron probe (dp) of 1.2 nm while, for thermal emission model the diameter of probe is about 10 nm (7). However, because the high costs and needed to high vacuum more than 10-10 Torr, as well as a high precision of alignments, the thermal emission model has been preferred in measurements due to the less costs and using low vacuum which is about 10-7 Torr (8,9). The electron microscope uses the accelerated electron that having a short wavelength less than 0.01 nm to improve the resolving power compared to the optical microscope that using a wavelength in the range of 300 nm to 700 nm. The numerical simulation program was suggested by Munro (9) using finite element's method to reduce the failed in manufacturing of electron lenses which have been widely applied.

The magnetic lens consists of a circle coil which is composed of N turns made of copper wire which is electrical insulated. When the continuous electric current (I) passes through the coil then a symmetrical axial magnetic field (Bz) will be produced a long Z axis. This field acts to deflect electron beam that passing through it towards the coil center according to Amper's law (10):

$$\int_{Z_0}^{Z_1} Bz\,dz = \mu_0 NI \qquad (1)$$

Where, $\mu_0 = 4\pi \times 10^{-7}$ H.m^{-1} represents the vacuum permeability and Bz is the axial magnetic flux density.

One of the main components in the electron microscope is the objective lens which acts to concentrate the electron beam that incident on specimen surface and limiting the resolving power in electron microscope. Therefore, it is considered the most important part that significantly contributing in reducing a spherical and chromatic aberration in the optical column by deflecting the electron beam strongly towards the optical axis (11).

In this paper, we report a design of an objective lens immersion type that having a high magnetic field density, small electron probe diameter and low aberrations.

2. Methodology

Munro 1973 (AMAG, M12, M13) were used to design and characterizing the optical properties and calculate the magnetic flux density and magnetic flux lines within the lens structure of designed immersion objective lens using the finite elements method (FEM)(4).

3. Results and Discussion

Figure 1 illustrates three different design of magnetic lens. Different iron arm thickness (4, 8, 12) mm were used in designing the lens at a constant distance between poles (S=2 mm). For clarification, the inner and outer diameters of the lens are about 10 mm and 86 mm respectively, the lens length is 53 mm and the dimensions of the lens coil are (30×30) mm for all lenses were designed. The colors (yellow, red and blue) represent respectively; coil, pole piece and the Yoke.

Figure 1. Three different design of objective magnetic lens with different iron arm thickness (t=4 mm, t= 8 mm and t= 12 mm) at constant distance between pole piece (S=2 mm).

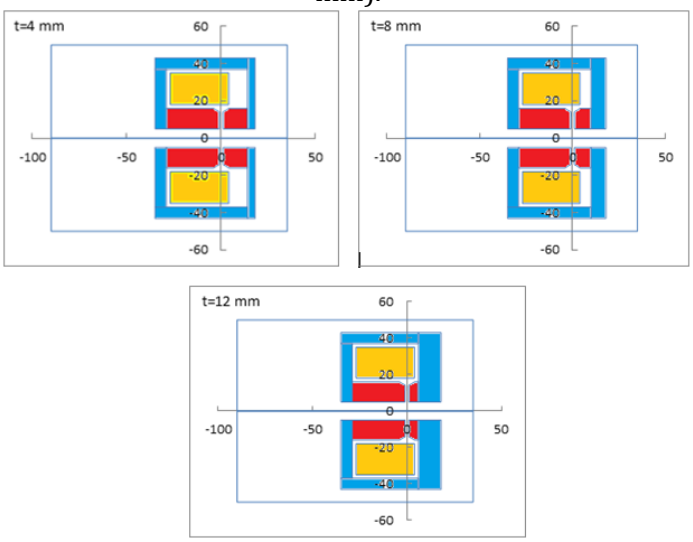

Figure 2 shows the distribution of magnetic flux lines inside the lenses showed in figure 1 using flux program (M13). These lines used to clarify and studying the behavior of lens and knowing the leaky magnetic flux in the lens.

Figure 2. The distribution of magnetic flux lines of three different design of objective magnetic lens with different iron arm thickness (t=4 mm, t= 8 mm and t= 12 mm) at constant distance between pole piece (S=2 mm).

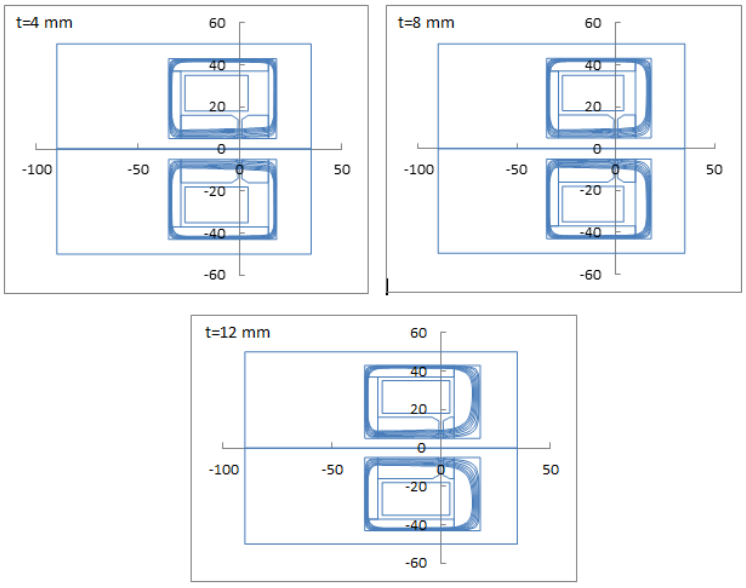

Figure 3 shows the distribution of axial magnetic flux density (Bz) at constant lens excitation (NI= 2 kA-t) as a function of optical axis. It can be noticed that the highest magnetic flux density is when the iron arm thickness equal to (8 mm), while, the flux is lowest at a thickness of 12 mm.

Figure 3. The axial magnetic flux density distribution (Bz) for all three lenses at a constant lens excitation (NI= 2 kA-t).

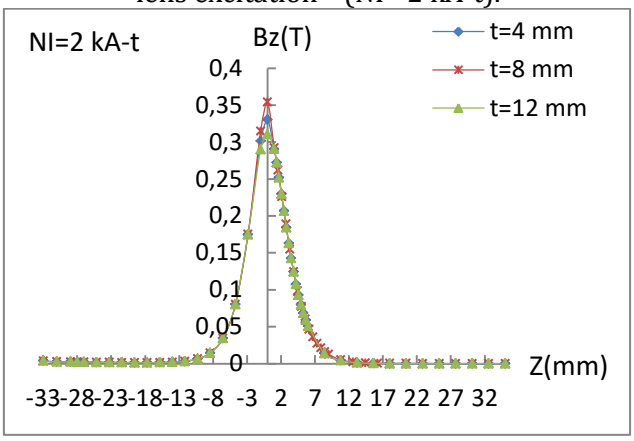

Figure 4 shows the focal length (fo), spherical aberration (Cs) and chromatic aberration (Cc) as a function of iron arm thickness of lenses at a constant lens excitation (NI= 2 kA-t) and acceleration voltage (Vr= 5 kV). It can be observed that the lens thickness of 8 mm has achieved lowest focal length and aberrations. All calculated values of optical properties are shown in table 1.

Figure 4. The focal length and aberration of three lenses.

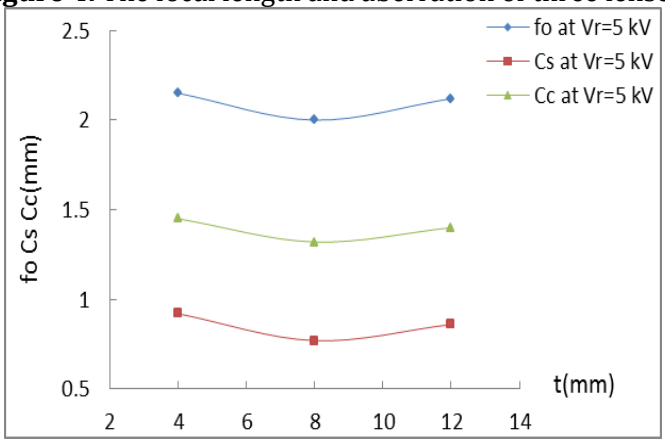

Table 1. The optical properties of all three lenses at a constant lens excitation (NI= 2 kA-t) and acceleration voltage (Vr= 5 kV).

Iron arm thickness (mm)	Focal length (mm)	Spherical aberration (mm)	Chromatic aberration (mm)	Magnetic Flux density(T)
4	2.13	0.92	1.45	0.316
8	2.0	0.77	1.32	0.354
12	2.11	0.86	1.40	0.310

It can be seen that the best lens was selected having the iron arm thickness of 8 mm which achieved a good optical properties; high flux density and low aberrations. Therefore, it was selected to study the effect of changing the distance between the pole piece of selected lens.

For The selected lens, the distribution of magnetic flux lines inside the lenses after Changing the distance between the pole piece of selected lens (S=2,4,6) mm at constant iron arm thickness (t=8 mm) using flux program (M13) is shown in figure

5. By this figure, it can be observed that, at lowest distance between the poles (2 mm), the highest density of magnetic flux lines is obtained which provides a low half width (HW) and highest magnetic flux density (0.354 T) of Bz. Thus, the optical properties were improved.

Figure 3. The distribution of magnetic flux lines of three different design of objective magnetic lens with different distance between pole piece (S=2 mm, S=4 mm, S=6 mm) at constant iron arm thickness (t= 8 mm).

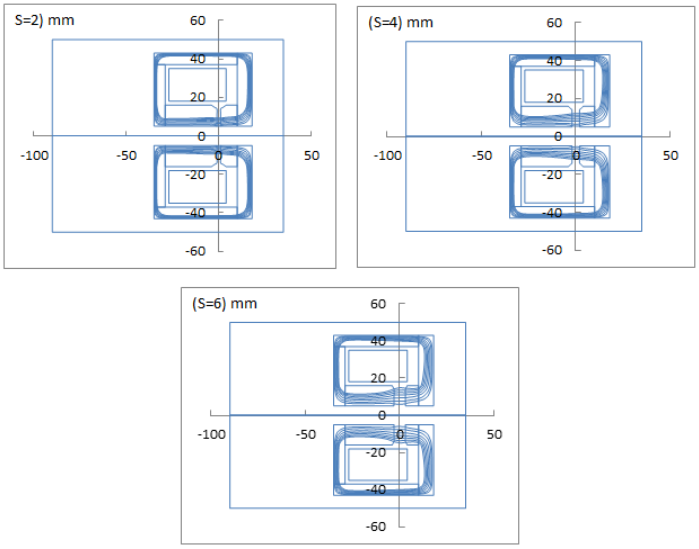

Figure 6 shows the distribution of axial magnetic flux density (Bz) at constant lens excitation (NI= 2 kA-t) as a function of optical axis. The highest magnetic flux density was obtained when the distance between pole piece equal to (2 mm), while, the flux is lowest at (6 mm).

Figure 6. The axial magnetic flux density distribution (Bz) for all three lenses at a constant lens excitation (NI= 2 kA-t).

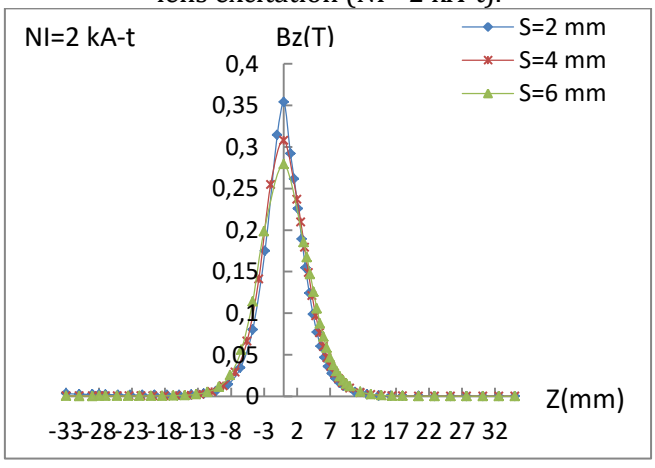

Figure 7 shows the optical properties of three lenses; focal length (fo), spherical aberration (Cs) and chromatic aberration (Cc) as a function of distance between pole piece of lenses at a constant lens excitation (NI= 2 kA-t) and acceleration voltage (Vr= 5 kV). It depicts that the lens having a 2 mm distance between poles has lowest focal length and aberrations. Table 2 demonstrates the calculated values of optical properties.

Figure 7. The focal length and aberration of three lenses.

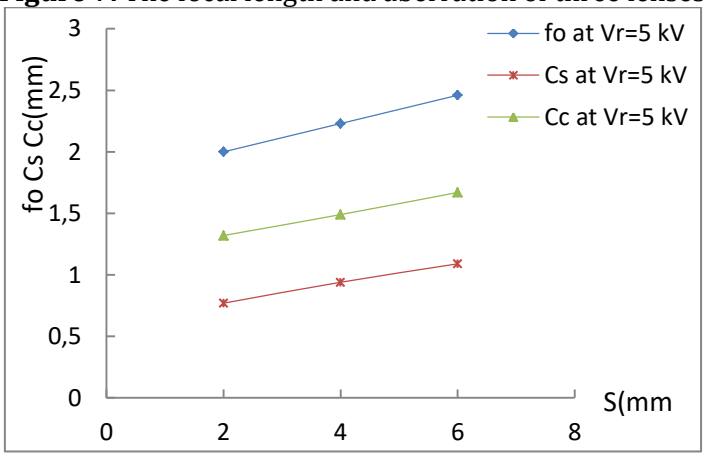

Table 2. The optical properties of all three lenses at a constant lens excitation (NI= 2 kA-t) and acceleration voltage (Vr= 5 kV).

Distance Between Pole piece (mm)	Focal length (mm)	Spherical aberration (mm)	Chromatic aberration (mm)	Magnetic Flux density(T)
2	2.0	0.77	1.32	0.354
4	2.23	0.94	1.49	0.308
6	2.46	1.09	1.67	0.279

The results that we obtained from the table above the lens which has the iron arm thickness and distance between pole piece 8 mm, 2 mm, achieved a good optical properties; high flux density and low aberrations. Therefore, it was selected as optimum lens to study its optical properties.

For the selected lens (iron arm thickness of 8mm, pole piece distance of 2 mm),the distribution of axial magnetic flux density (Bz) at different lens excitation (NI=500, 1000, 1500, 2000) A-t as a function of optical axis is illustrated in figure 8. This figure revealed that the highest magnetic flux density was obtained when the distance between pole piece equal to (2 mm), while, it is lowest at a distance of (6 mm).

Figure 8. The axial magnetic flux density distribution (Bz) for selected lens at a different lens excitation.

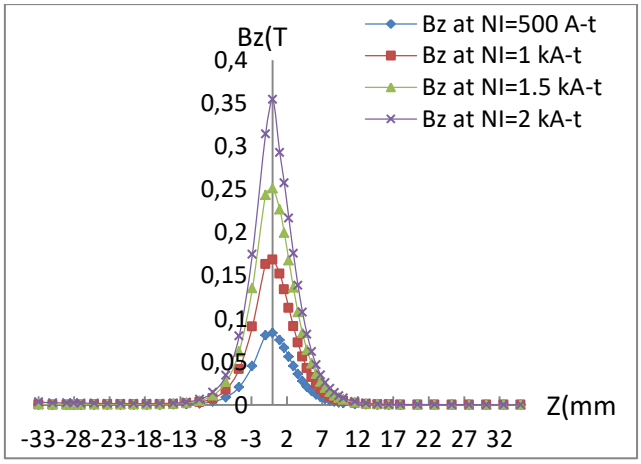

Figure 9 illustrate the maximum values of distribution of axial magnetic flux density (Bz) shown in figure 8 as a function of a different lens excitation (NI=500, 1000, 1500, 2000) A-t. It shows that the magnetic flux density increase increases when the lens excitation was increased.

Figure 9. Distribution of axial magnetic flux density (Bz) as a function of a different lens excitation.

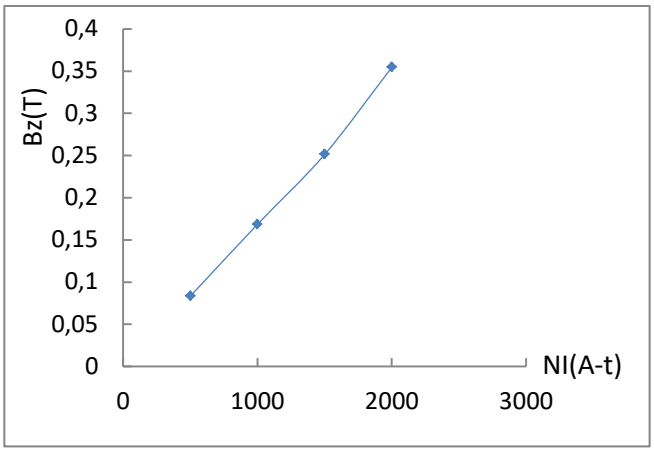

Figure 10 shows the relation between the optical properties and the excitation parameter (NI/SQRT (Vr)). It can be seen that the all optical properties (fo, Cs, and Cc) have gradually decreased by increasing the excitation parameter at a constant lens excitation of 2 kA-t. However, they remain approximately constant when the parameter becomes larger than 35.

Figure 10. The relation between the optical properties and the excitation parameter of selected lens.

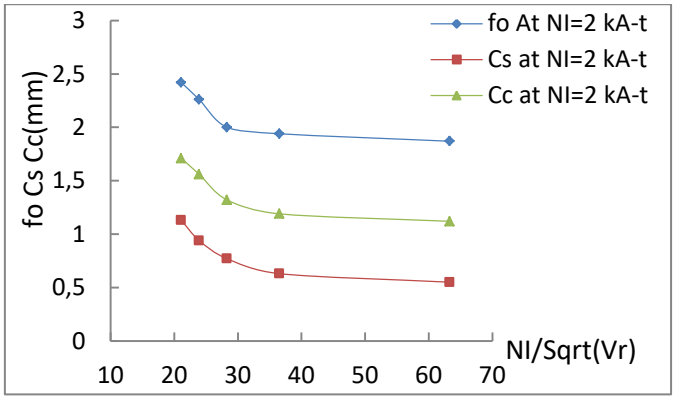

A range of acceleration voltage between 1 kV to 9 kV (2 kV step) was used to accelerate the electrons inside the selected lens. Figure 11 demonstrates the relation between the optical properties and the acceleration voltage. It can be observed that increasing the acceleration voltage causes increasing in the optical properties (fo, Cs, Cs). This increasing leads to image distortion which is considered as disadvantages of using a high acceleration voltage. Therefore, avoiding a high acceleration voltage is required while using the magnetic lens.

Figure 11. The relation between the optical properties and acceleration voltage of lens.

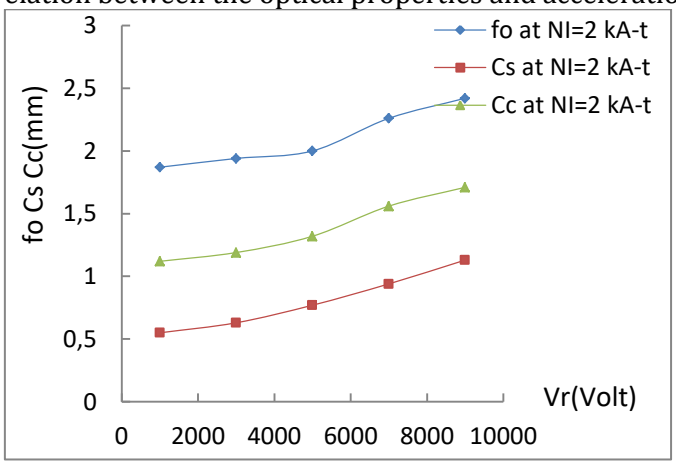

4. Conclusion

This paper shows the effect of iron arm thickness and the distance between the pole pieces of magnetic lens on the performance of the lens. This paper shows a direct effect of changing the iron arm thickness and the distance between the poles on the optical properties of the lens, therefore, a specific arm thickness of 8 mm and poles distance of 2 mm were choice for the best performance of the lens as it gives an optimum optical properties than other thicknesses and pole distances were used in this study.

References

1. Khursheed A. Magnetic axial field measurements on a high resolution miniature scanning electron microscope. Rev Sci Instrum. 2000;71(4):1712–5.
2. Stephen J. Pennycook (auth.), Stephen J. Pennycook PDN (eds. . Scanning Transmission Electron Microscopy Imaging and Analysis. Pennycook SJ, Technology MS and, editors. USA; 2011. 755 p.
3. Hussein MA. Numerical analysis to verifying the performance of condenser magnetic lens in the scanning electron microscope . 2016;58(2005):44–9.
4. Abbass TM, a NB. Study of the Objective Focal Properties for Asymmetrical Double Polepiece Magnetic Lens. Br J Sci [Internet]. 2012;6(2):43–50. Available from: http://www.uobabylon.edu.iq/uobcoleges/service_showarticle.aspx?fid=21&Pubid=4455
5. Egerton RF. Physical Principles of Electron Microscopy. Phys Princ Electron Microsc. 2016;
6. Khursheed A. Scanning electron microscope optics and spectrometer. Singapore: World Scientific Publishing Co. Pte. Ltd; 2011.
7. Graciela W. Padua QW. Nanotechnology Research Methods for Foods and Bioproducts. First Edit. USA: A John Wiley & Sons, Ltd., Publication; 2012. 261 p.

8. Joseph Goldstein, Dale E. Newbury, David C. Joy, Charles E. Lyman, Patrick Echlin, Eric Lifshin, Linda Sawyer JRM. Scanning Electron Microscopy and X-ray Microanalysis: Third Edition. 2012;690. Available from: http://discovery.ucl.ac.uk/59147/

9. Hussein MA. Effect of the Geometrical Shape of the Magnetic Poles and the Distance between Them on the Focal Properties of the Condenser Magnetic Lens in the Scanning Electron Microscope (SEM). 2016;4(5):130–4.

10. Peter Hawkes EK. Principles of Electron Optics. Principles of Electron Optics. 2018.

11. Fujita FE, Hirabayashi M. High-Resolution Electron Microscopy. Microsc Methods in Met. 2009. 29–74 p.